TWIST MORPHING OF A HINGELESS ROTOR BLADE USING A MOVING MASS

M.R. Amoozgar, A.D. Shaw, J. Zhang, M.I. Friswell

College of Engineering, Swansea University, Swansea, Wales SA2 8PP, United Kingdom

Abstract

This paper presents a new concept of morphing by changing the twist of a composite blade through the movement of a mass near the tip of the blade. The mass is moved in the chordwise direction which then modifies the centrifugal force near the tip of the blade. The blade is tailored with composite materials and hence coupling is introduced. By moving the mass in the chordwise direction, a variable bending moment is produced which is the result of the offset between the point mass centrifugal force and the shear centre of the blade section. This bending moment will be transferred to the composite spar, and then through the bend-twist coupling of the composite layup, a variable torsional moment will be induced. This variable torsional moment changes the twist distribution of the blade. The dynamics of the rotating composite blade is modelled by using the geometrically exact fully intrinsic beam equations and the point mass is considered as a non-structural concentrated mass which has offsets with respect to the beam reference line. It is found that by moving the mass in the chordwise direction, the twist distribution of the blade changes. The rate of twist change completely depends on the bend-twist coupling and also the point mass magnitude and location. Finally, the effect of sensitive morphing parameters on the rotating frequencies of the Bo105 main rotor blade is determined.

Nomenclature

$\mathbf{A,B,D}$	Cross-section stiffness matrix components
$\mathbf{C}$	Rotation matrix
$\mathbf{c}$	Chord length
$\mathbf{F, M}$	Internal force and moment
$\mathbf{K}$	Final curvature
$\mathbf{P, H}$	Sectional linear and angular momenta
R	Blade length
$\mathbf{r}$	Position vector
$\mathbf{u}$	Displacement vector
$\mathbf{V, \Omega}$	Linear and angular velocities
x_p, y_p	Point mass location along x and y directions
α	Bend-twist coupling index
μ	point mass ratio
θ	Twist value
$\boldsymbol{\gamma, \kappa}$	Strain measures

1. INTRODUCTION

Rotorcraft have many advantages over fixed wing aircraft. Today's rotorcraft need to improve to be more environmentally friendly in terms of low levels of noise, pollution, fuel consumption, and high levels of performance and comfort. To achieve this aim, adaptive helicopters are a candidate solution, and some new concepts have been proposed. These concepts all promise to enhance the performance, or to reduce the noise and vibration of the rotorcraft by changing the shape of the blade which then modifies the aerodynamic domain. Among all possible concepts for morphing a blade, the twist and trailing edge flap concepts have received the most attention over the past two decades [1]. Several different ideas for the control of a blade, including twist, pitch, flap, and camber, have been reviewed by Straub and Chopra, and the advantages and disadvantages of these methods for vibration reduction has been reported [2, 3]. The change in the blade twist during flight is the focus of this paper. When a rotorcraft is in the hover condition, highly twisted blades are optimal, while low levels of twist are optimal for high-speed forward velocities [4]. Therefore, the predefined blade twist variation normally is chosen as a compromise between different flight conditions. Blade twist morphing changes the blade twist actively during flight to allow the rotorcraft to fly in an optimum condition in terms of twist variation. Han et al. [5] showed how the performance of a helicopter during flight could be improved by dynamic blade twist. They demonstrated that the dynamic blade twist improves the performance and reduces the rotor power requirement.

Presented at 44th European Rotorcraft Forum, Delft, The Netherlands, 19-20 September, 2018

One of the earliest studies concerning the twist change of the blade via piezoelectric actuators was performed by Chen and Chopra [6]. In this study, the piezoelectric patches were located on the lower and upper surfaces of the blade, and about 0.4^o of twist change was achieved at 4 per rev. This concept was tested in the hover and it was found that a linear twist change of about 0.6^o may result in a 10% increase in the rotor lift [7]. Chattopadhyay et al. [8] used smart materials to reduce and control the vibratory load of a composite box beam blade. They showed that the number of actuators and their location significantly affects the blade dynamic load reduction. The dynamic behaviour of active twist rotor blades with distributed anisotropic strain actuators for vibration and noise reduction purposes has been investigated experimentally and analytically by Cesnik et al. [9]. Good correlation between their developed analytical model and the experimental results has been reported. This study was continued to check the developed analytical model for the forward flight condition by Shin and Cesnik [10]. Thakkar and Ganguli [11] considered the vibration reduction of a soft in plane hingeless rotor blade in forward flight with induced shear based on piezoceramic actuation. They showed that about 43% reduction in the vibration is feasible. Schultz [12] proposed a new concept capable of large shape morphing with a small energy input based on bi-stable structures. The active vibration reduction of composite hingeless rotor blades with dissimilarity based on the active twist concept has been investigated by Prashant and Sung [13]. The numerical results showed that the blade dissimilarities influence the rotor vibratory loads and the input energy. You et al. [14] examined the influence of different actuation scenarios for maximizing the performance of a rotor in the high-speed flight conditions. Apart from using piezo materials for blade morphing, there are some other efforts focusing on using shape memory alloys for blade twist change. Prahlad and Chopra [15] presented the concept of using a shape memory alloy torque tube to change the twist distribution of a tiltrotor blade between hover and forward flight. The effect of heat treatment of the SMAs in tuning the actuation behaviour was discussed. The development and experiment of an active twist rotor blade using a thermo-mechanical shape memory alloy has been reported by Bushnell et al. [16]. In the ONR-funded Reconfigurable Rotor Blade program the SMA actuator has been used to change the twist of a V-22 Osprey blade [17-19]. It was shown that about 2^o of twist change is feasible with this SMA concept [18]. Pagano et al [20] proposed a SMA rod mechanism for morphing helicopter blades to mitigate the environmental impact. There are also other concepts in the literature for changing the twist of the blades. One concept for twist variation of the blade is the warp-induced twist which originally was proposed for fixed-wing applications [21], and then extended to rotary-wings [4]. In this concept, the ribs can rotate freely around the spar, and the skin is also free to move on the ribs. The warping is generated by creating a relative motion in the span-wise direction by using a threaded rod, and when this rod rotates the result is a twist change of the blade.

In addition to all the concepts of twist morphing, in this paper a new concept for changing the twist of a composite blade is introduced and examined. In this concept the change of the blade twist is obtained by moving a mass near the tip of the blade to create a local centrifugal force which then, through the bending -twist coupling of the composite layup, results in a torsional moment. This torsional moment is then able to change the twist angle of the blade cross-section. In this paper, the proposed concept is first introduced, and the important parameters are summarized. Then an analytical model capable of examining this concept on a composite blade is developed, and the effect of different system parameters and their influence on the twist of the blade are presented**.**

2. CONCEPT DESCRIPTION

The proposed method for morphing a composite blade is controlled by means of a moving mass. This is done by moving a mass in the chordwise direction of the cross-section of the composite blade. This concentrated mass and the blade rotational velocity produces an extra centrifugal force that can change the twist of the blade through the bend-twist coupling of the composite layup.

Figure 1 schematically shows this twist morphing concept. The point mass, whose location is denoted by x_p, and y_p, moves in the chordwise direction to produce a bending moment which is the result of the offset of the centrifugal force acting on the mass from the section shear centre. This bending moment may result in an equivalent torsional moment through the bend-twist coupling of the composite layups. Then the twist distribution of the blade can be changed because of this induced torsional moment. Therefore, the point mass movement actuates the twist of the blade. It is noted that the point mass moves along the chord of the blade in a guided predefined direction attached to the blade so that the moment due to the point mass can be transferred to the blade.

Presented at 44th European Rotorcraft Forum, Delft, The Netherlands, 19-20 September, 2018

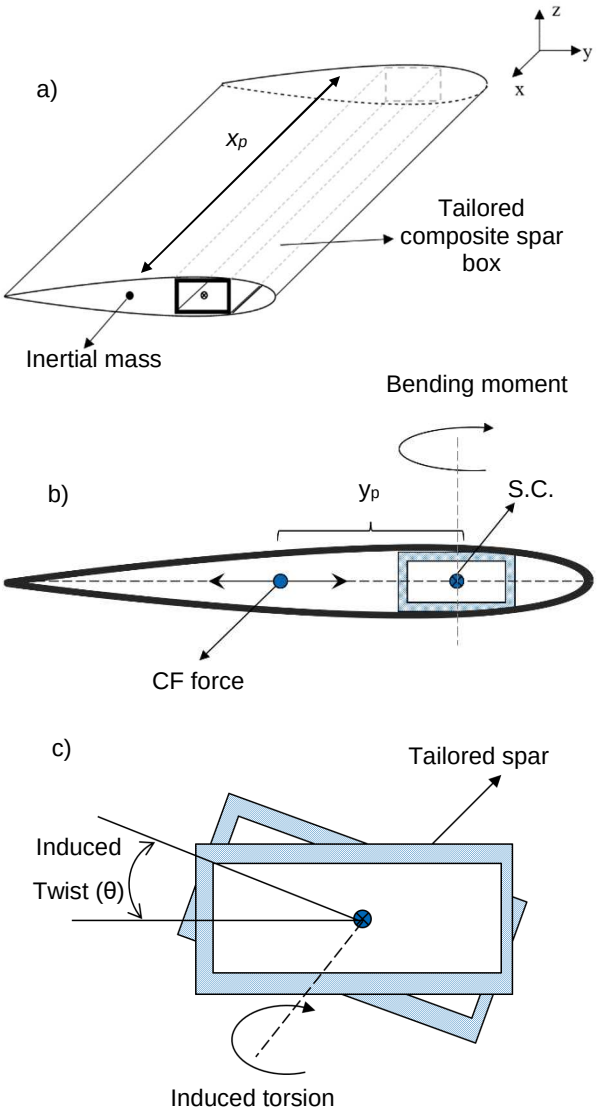

Figure 1: Schematic description of the twist morphing concept a) spanwise position of the mass b) chordwise position of the mass c) twisted section

3. MODELLING

The hingeless rotor blade is modelled here as an elastic beam cantilevered to the rotor hub, and the point mass is simulated as a concentrated non-structure mass located at an arbitrary location. The 1D beam behaviour is simulated by using the geometrically exact fully intrinsic beam equations [22]. This formulation is free of displacement and rotation variables and determines the dynamics of a curved anisotropic beam. This beam model has been used for modelling beam like structures successfully ([23-26]). Thus:

$$\partial F_1/\partial x_1 + K_2F_3 - K_3F_2 = \partial P_1/\partial t + \Omega_2P_3 - \Omega_3P_2$$

$$\partial F_2/\partial x_1 + K_3F_1 - K_1F_3 = \partial P_2/\partial t + \Omega_3P_1 - \Omega_1P_3$$

$$\partial F_3/\partial x_1 + K_1F_2 - K_3F_1 = \partial P_3/\partial t + \Omega_1P_2 - \Omega_2P_1$$

$$\frac{\partial M_1}{\partial x_1} + K_2M_3 - K_3M_2 + 2\gamma_{12}F_3 - 2\gamma_{13}F_2 = \partial H_1/\partial t + \Omega_2H_3 - \Omega_3H_2 + V_2P_3 - V_3P_2$$

$$\partial M_2/\partial x_1 + K_3M_1 - K_1M_3 + 2\gamma_{13}F_1 - (1+\gamma_{11})F_3 = \partial H_2/\partial t + \Omega_3H_1 - \Omega_1H_3 + V_3P_1 - V_1P_3$$

$$\frac{\partial M_3}{\partial x_1} + K_1M_2 - K_2M_1 + (1+\gamma_{11})F_2 - 2\gamma_{12}F_1 = \partial H_3/\partial t + \Omega_1H_2 - \Omega_2H_1 + V_1P_2 - V_2P_1$$

$$\frac{\partial V_1}{\partial x_1} + K_2V_3 - K_3V_2 + 2\gamma_{12}\Omega_3 - 2\gamma_{13}\Omega_2 = \partial\gamma_{11}/\partial t$$

$$\frac{\partial V_2}{\partial x_1} + K_3V_1 - K_1V_3 - (1+\gamma_{11})\Omega_3 + 2\gamma_{13}\Omega_1 = 2\partial\gamma_{12}/\partial t$$

$$\frac{\partial V_3}{\partial x_1} + K_1V_2 - K_2V_1 + (1+\gamma_{11})\Omega_2 - 2\gamma_{12}\Omega_1 = 2\partial\gamma_{13}/\partial t$$

$$\partial\Omega_1/\partial x_1 + K_2\Omega_3 - K_3\Omega_2 = \partial\kappa_1/\partial t$$

$$\partial\Omega_2/\partial x_1 + K_3\Omega_1 - K_1\Omega_3 = \partial\kappa_2/\partial t$$

(1) $$\boldsymbol{\partial\Omega_3/\partial x_1 + K_1\Omega_2 - K_2\Omega_1 = \partial\kappa_3/\partial t}$$

Where F_i and M_i for i=1,..,3, are the internal forces and moments, V_i and Ω_i are the linear and angular velocities, P_i and H_i are the sectional linear and angular momenta, respectively. The strains of the blade are denoted by γ_{1i} and κ_i and K_i is the final curvature of the deformed beam. All of the variables are measured in the deformed beam except for the initial curvature. The internal forces and moments are related to the generalized strains by using the stiffness matrix as:

(2)
$$\begin{bmatrix} F_1 \\ F_2 \\ F_3 \\ M_1 \\ M_2 \\ M_3 \end{bmatrix} = \begin{bmatrix} A_{11} & A_{12} & A_{13} & B_{11} & B_{12} & B_{13} \\ A_{12} & A_{22} & A_{23} & B_{21} & B_{22} & B_{23} \\ A_{13} & A_{23} & A_{33} & B_{31} & B_{32} & B_{33} \\ B_{11} & B_{12} & B_{13} & D_{11} & D_{12} & D_{13} \\ B_{21} & B_{22} & B_{23} & D_{12} & D_{22} & D_{23} \\ B_{31} & B_{32} & B_{33} & D_{13} & D_{23} & D_{33} \end{bmatrix} \begin{bmatrix} \gamma_{11} \\ 2\gamma_{12} \\ 2\gamma_{13} \\ \kappa_1 \\ \kappa_2 \\ \kappa_3 \end{bmatrix}$$

$$\Longrightarrow \begin{bmatrix} \boldsymbol{F} \\ \boldsymbol{M} \end{bmatrix} = \begin{bmatrix} \boldsymbol{A} & \boldsymbol{B} \\ \boldsymbol{B^T} & \boldsymbol{D} \end{bmatrix} \begin{bmatrix} \boldsymbol{\gamma} \\ \boldsymbol{\kappa} \end{bmatrix}$$

where **A**, **B**, and **D** are the stiffness components of the composite blade cross-section. All the cross-sectional quantities mentioned above are calculated by using the cross-sectional analysis software, VABS, which has been extensively

Presented at 44th European Rotorcraft Forum, Delft, The Netherlands, 19-20 September, 2018

validated and used in composite beam applications [27]. It is noted that here the bending-torsional coupling (D_{13}) is of great interest. It is noted that in this case with the data available, only 4 stiffness terms are used, the torsional stiffness (D_{11}), the chordwise stiffness (D_{22}), the flapwise stiffness (D_{33}), and the bending-torsional coupling stiffness (D_{13}).

To close the composite blade equations, it is necessary to define the boundary conditions of the blade. In this study, it is assumed that the blade is a hingeless rotor blade which is completely fixed at the rotor hub.

To solve the governing equations of the blade, a space-time discretization scheme has been used [22]. In this method, any variable in the equations of motion are defined on the left and right sides of each node. This is appropriate to take into account any discontinuity such as the point mass. Finally, the equations of motion are summarized in a compact form as

$$a_{ji}\dot{\mathrm{q}}_i + b_{ji}\mathrm{q}_i + c_{jik}\mathrm{q}_i\mathrm{q}_k = 0 \quad (3)$$

where $\mathbf{q}$ is the vector containing the unknown parameters (F_i, M_i, V_i, Ω_i, i=1..3) at the left and right side of each node, and a_{ji}, b_{ji}, c_{jik} are the matrices of linear and nonlinear coefficients. The steady state condition of the system is determined by removing all time derivative terms and solving the resultant nonlinear equations by the Newton-Raphson method. Then the natural frequencies of the system are determined from the eigenvalue analysis of the linearized system about the steady state condition. It is noted that as the fully intrinsic formulation is free of displacement and rotation variables, to recover these variables the following equations can be used:

$$\begin{aligned} \partial\mathbf{C}/\partial x_1 &= -(\tilde{\mathbf{k}} + \tilde{\boldsymbol{\kappa}})\mathbf{C} \\ \partial(\mathbf{r}+\mathbf{u})/\partial x_1 &= \mathbf{C}^T(\boldsymbol{\gamma} + \boldsymbol{e_1}) \end{aligned} \quad (4)$$

where $\mathbf{u}$ is the displacement vector, $\mathbf{r}$ is the position vector in the undeformed reference frame, $\boldsymbol{C}$ is the rotation matrix, and $\mathbf{e}_1$ is a vector can be defined as $\mathbf{e}_1 = [1\ 0\ 0]^T$. Furthermore, $(\tilde{\ })$, the tilde operator converts any arbitrary vector such as $\mathbf{Z} = [Z_1 \quad Z_2 \quad Z_3]^T$ to its equivalent matrix as follow

$$\tilde{\mathbf{Z}} = \begin{bmatrix} 0 & -Z_3 & Z_2 \\ Z_3 & 0 & -Z_1 \\ -Z_2 & Z_1 & 0 \end{bmatrix} \quad (5)$$

4. RESULTS

A pre-twisted hingeless rotor blade that resembles the main rotor blade of BO-105 with the characteristics reported in Table 1 is considered ([28]).

Table 1: Parameters of the BO-105 main rotor blade

Item	Value
Radius (m)	4.91
Chord (m)	0.27
Pre-cone angle (deg)	2.5°
Rotating velocity (rad/s)	44.4

Unlike the BO-105 blade that has variable spanwise properties, here it is considered that the blade has uniform spanwise properties. The cross-sectional properties of the equivalent uniform blade are selected so that the fundamental frequencies of the blade be as close as possible to the BO-105 blade.

Table 2: Comparison of the equivalent blade frequencies with those of the BO-105 blade

Mode	Present (Hz)	Peterson et al. [28] (HZ)
1st Lag	4.61	4.66
1st Flap	7.52	7.91
2nd Flap	20.03	19.64
1st Torsion	25.40	26.78
2nd Lag	29.8	30.6

To achieve this aim a GA optimization algorithm is used. The comparison between the fundamental frequencies of the equivalent blade and the BO-105 blade are reported in Table 2. From here on, all the results are based on the equivalent blade.

As mentioned before, the bend-twist coupling is the source of morphing in this concept. Therefore, here it is considered that the bend-twist stiffness term, e.g. D_{13}, exists and is related to the torsional stiffness (D_{11}) and bending stiffness (D_{33}) through the following relation:

$$D_{13} = \alpha.\sqrt{D_{11}.D_{33}} \quad (6)$$

where, α is the nondimensional bend-twist coupling index which may have a value between -1≤α≤1 [29]). It is assumed here that this term is added to the blade stiffness matrix without altering other properties.

A non-structural mass is added to the blade to produce an extra centrifugal force which then can change the twist of the blade through the bend-twist coupling. The concentrated mass is considered to be a fraction of the blade mass itself as follows

$$\mu = \frac{m_p}{m.R} \quad (7)$$

Presented at 44th European Rotorcraft Forum, Delft, The Netherlands, 19-20 September, 2018

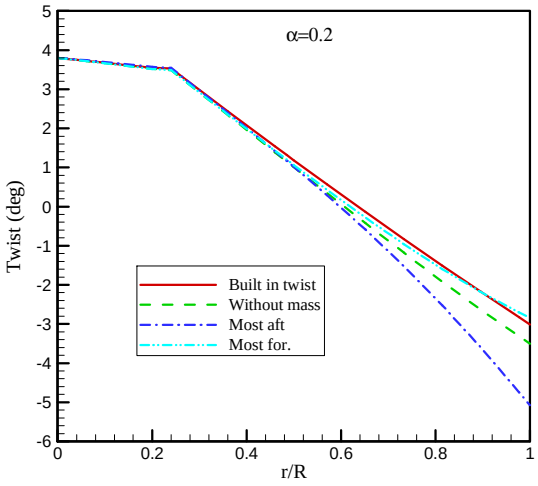

Figure 2: Twist change of the blade for μ=0.05 and α=0.2

Figure 2 shows the twist distribution of the blade for three different chordwise positions of the mass, when the spanwise location of the mass is at the tip of the blade, and the bend-twist coupling index is α=0.2. In this case 5 percent extra mass is added to the blade (μ=0.05). The solid line shows the build in pre-twist of the blade which is almost linearly distributed along the span. The dashed line represents the twist distribution when the blade is rotating with its nominal speed. The other two lines present the twist modification for mass movement from the leading edge to the trailing edge. Clearly, by adding the mass to the blade, the twist distribution of the blade can be modified. In this case by moving the mass from the leading edge to the trailing edge of the section about 2^o twist change is induced at the tip of the blade. It is noted that the modified twist distribution is not linear in this case and it has an almost quadratic distribution along the blade.

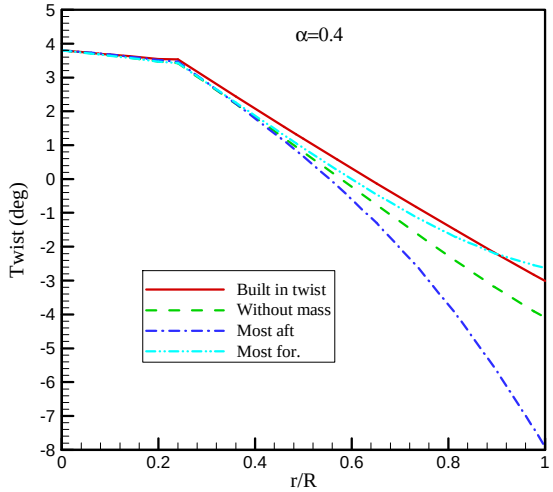

Figure 3: Twist change of the blade for μ=0.05 and α=0.4

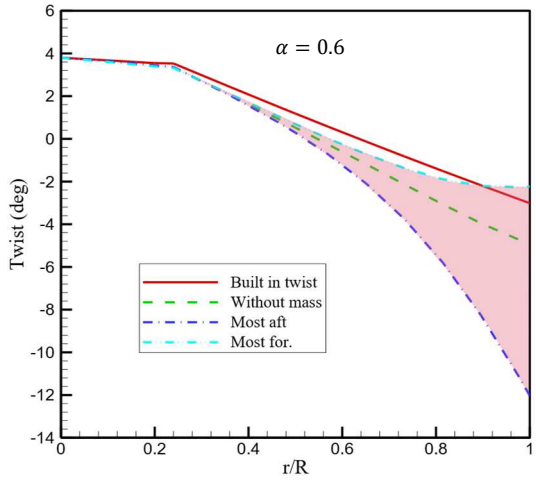

Figure 4: Twist change of the blade μ=0.05 and α=0.6

Figure 3 and 4 show the twist distribution of the blade for α=0.4 and α=0.6, respectively. By increasing the bend-twist coupling term, the amount of twist change increases. For the case of α=0.6, by moving the mass from the leading edge to the trailing edge of the blade, about 10^o tip twist change is induced in the blade. The blade can have any values of twist within the solid filled area showed in Figure 4. It is noted that the mass movement will affect the stability characteristics of the blade and therefore care must be taken in the selection of the point mass value and position.

The effect of spanwise location of the concentrated mass on the tip twist change of the blade is shown in Figure 5.

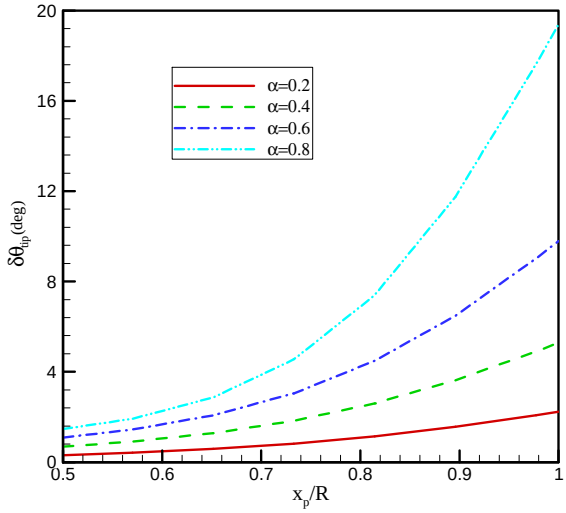

Figure 5: Twist change of the blade for different spanwise locations of the mass and different bend-twist coupling for μ=0.05

Here again the mass ratio is μ=0.05, and the tip twist change is determined from the difference between the tip twist when the mass is at the leading edge and the trailing edge. By moving the mass toward the tip of the blade, the twist change

Presented at 44th European Rotorcraft Forum, Delft, The Netherlands, 19-20 September, 2018

increases. This is true for all coupling values. This can be explained as the amount of centrifugal force that acts on the mass. By moving the mass toward the tip, more centrifugal force is induced in the system. Therefore, by locating the mass at or near the tip of the blade, more twist change is achieved.

The effect of the point mass ratio on the tip twist change of the blade for different coupling index is presented in Figure 6. By adding more mass to the blade, a higher twist change is achieved. On the other hand, the effect of the coupling index value is very important to induce the twist in the blade.

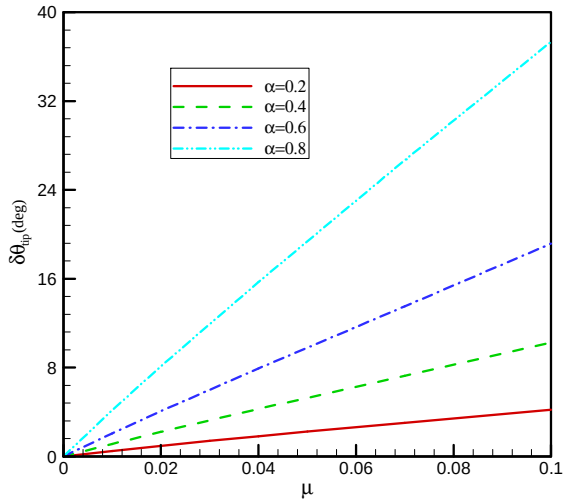

Figure 6: Tip Twist change of the blade for different coupling values

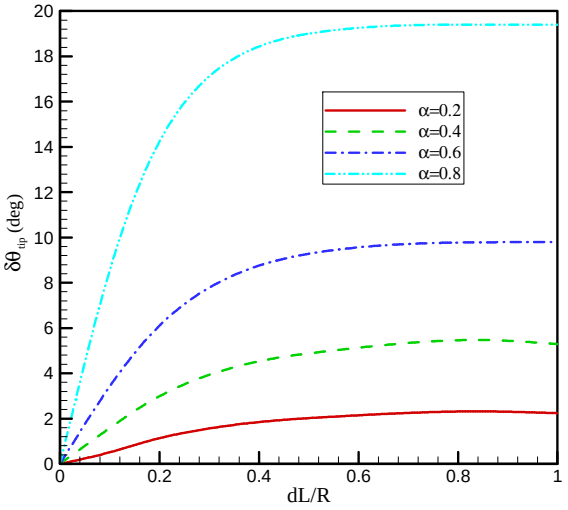

Figure 7: Tip twist change of the blade for different tailored length and different bend-twist coupling for μ=0.05

In the previous cases it was considered that the whole rotor blade is tailored. Now it is assumed that only a portion of the blade from the tip is made of composite materials. In this case, a segment of the blade with length *dL* from the tip is tailored and the effect of mass movement on the tip twist change is shown in Figure 7. By checking this plot, it is obvious that by increasing the length of the tailored segment, the tip twist change increases monotonically until the point about dL/R=0.4, and from here on the value of tip twist doesn't change significantly. So, for instance when the coupling index is α=0.6, by tailoring 40% of the blade, about $\delta\theta_{tip}$=9° of twist change is induced in the system by moving the mass from the tip to the root of the blade.

Adding a non-structural mass to the blade changes the dynamics of the blade, and in the following the effect of different effective parameters of the concept on the fundamental frequencies of the blade is examined.

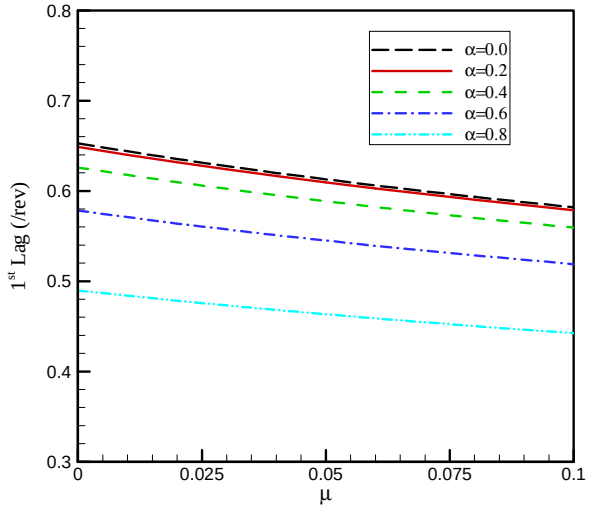

Figure 8: First lag rotating frequency variation for various mass ratios and different coupling values when y_p/c =0.0, x_p/R=1

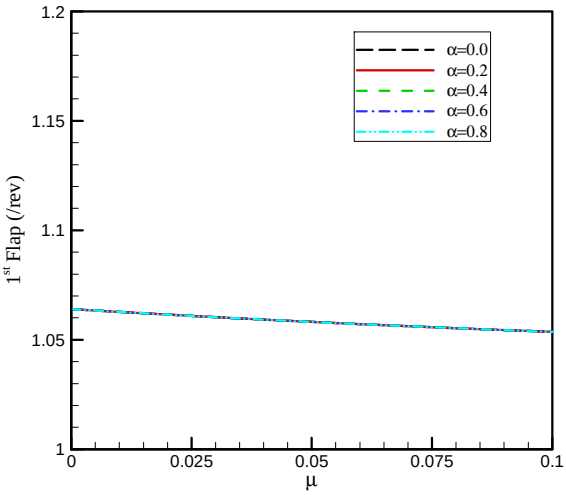

Figure 9: First flap rotating frequency variation for various mass ratios and different coupling values when y_p/c =0.0, x_p/R=1

Presented at 44th European Rotorcraft Forum, Delft, The Netherlands, 19-20 September, 2018

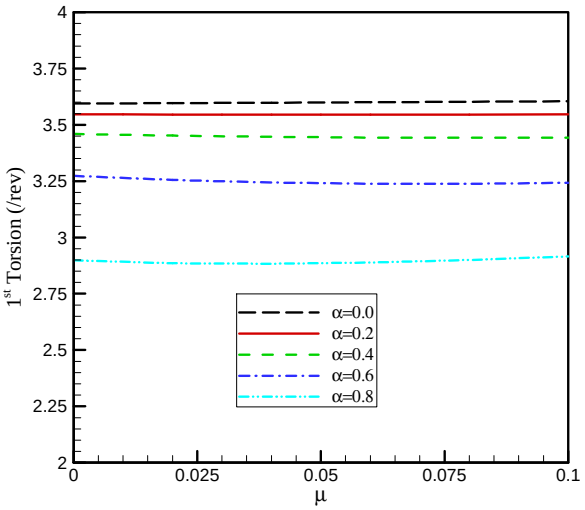

Figure 10: First torsion rotating frequency variation for various mass ratios and different coupling values when y_p/c =0.0, x_p/R=1

Figures 8 to10 show the effect of the added mass ratio on the frequencies of the first lag, flap, and torsion modes. By increasing the point mass ratio, the lag rotating frequency decreases continually, while the flap mode changes slightly. The torsion mode seems to be insensitive to the mass ratio for lower coupling values, but for higher bend-twist coupling the frequency changes slightly. Furthermore, the bend-twist coupling index affects the lag and torsion modes, but it doesn't have much effect on the lag mode.

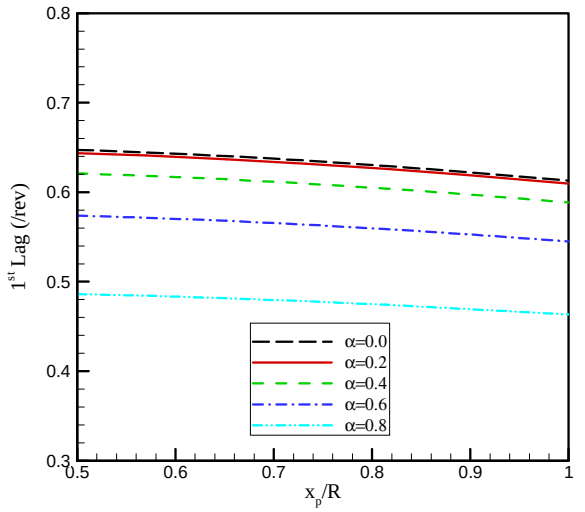

Figure 11: First lag rotating frequency variation for various mass spanwise position and different coupling values when y_p/c =0.0, μ=0.05

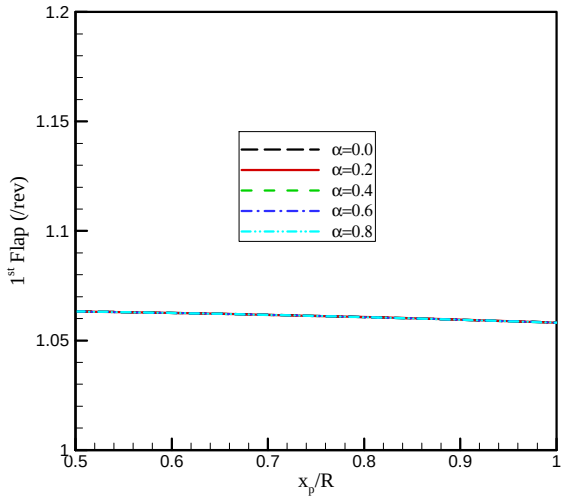

Figure 12: First flap rotating frequency variation for various mass spanwise position and different coupling values when y_p/c =0.0, μ=0.05

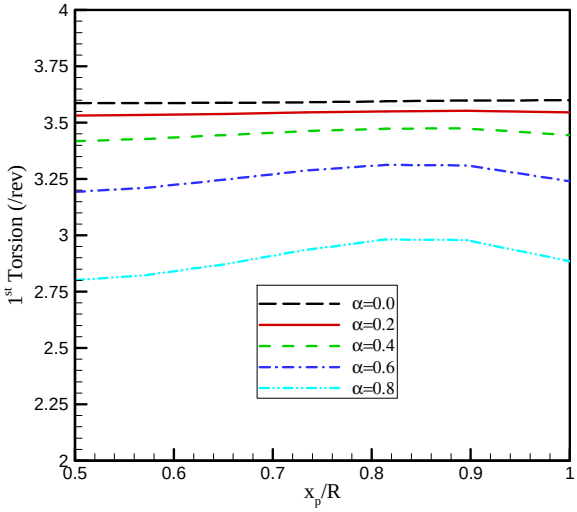

Figure 13: First torsion rotating frequency variation for various mass spanwise position and different coupling values when y_p/c =0.0, μ=0.05

Next the effect of spanwise location of the mass on the fundamental rotating frequencies is considered and shown in Figures 11 to 13. Again, the mass doesn't affect the lag mode significantly. By moving the mass from the middle of the blade to the tip, the flap mode frequency decreases gradually. On the other hand, by moving the mass in the spanwise direction, the torsional frequency first increases and then decreases. This point of change is different for different values of bend-twist coupling.

The effect of chordwise position of the point mass on the fundamental rotating frequencies is determined and shown in Figures 14 to 16. The chordwise location of the mass doesn't alter the first lag and flap frequencies. By moving the mass from the trailing edge to the leading edge of the blade, the torsional rotating frequency first decreases and then increases, but the rate of change is not very much.

Presented at 44th European Rotorcraft Forum, Delft, The Netherlands, 19-20 September, 2018

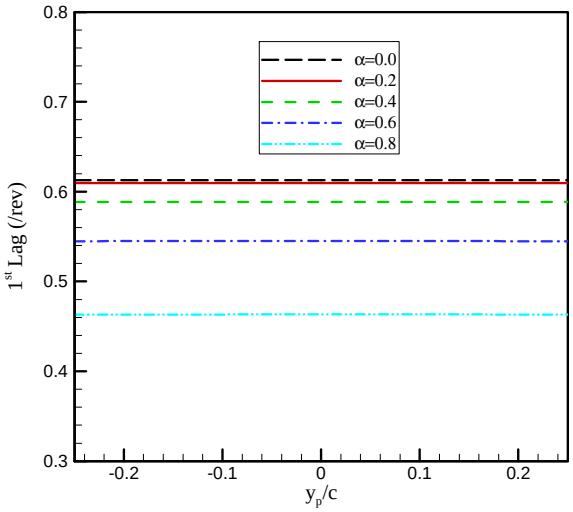

Figure 14: First lag rotating frequency variation for various mass chordwise position and different coupling values when x_P/R =1, μ=0.05

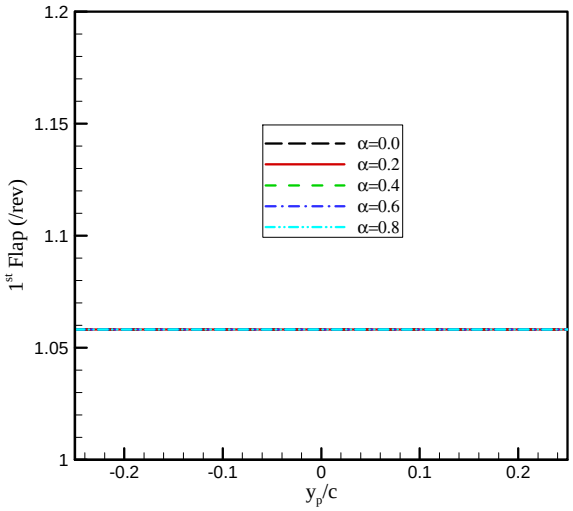

Figure 15: First flap rotating frequency variation for various mass chordwise position and different coupling values when x_P/R =1, μ=0.05

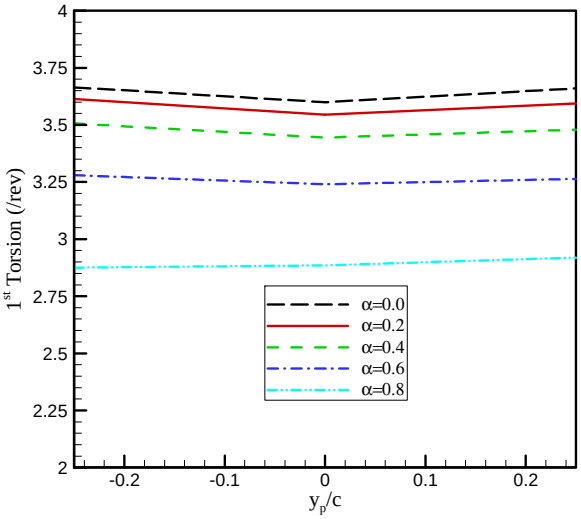

Figure 16: First torsion rotating frequency variation for various mass chordwise position and different coupling values when x_P/R =1, μ=0.05

5. CONCLUSION

In this paper, a new twist morphing concept is introduced. The twist change is the result of movement of a non-structural mass through the chord of the blade section. When the added mass moves along the chord of the blade, a bending moment is induced on the blade structure. If the blade structure designed to have bend-twist tailoring, this bending moment can change the twist of the blade. To investigate the concept, a hingeless rotor blade resembling the main rotor blade of the BO-105 is considered. The blade is modelled by using the geometrically exact fully intrinsic beam equations. A bend-twist coupling is introduced in the cross-sectional properties of the blade. The effect of different effective parameters on the twist change and fundamental rotating frequencies of the blade are investigated. It is found that the point mass magnitude and location along the span and chord of the blade affect the blade twist dramatically. It is also highlighted that the bend-twist coupling has an important contribution to the blade twist. By tailoring about 40% of the blade, a significant amount of twist change is induced in the blade. Finally, it is shown that the mass ratio, spanwise and chordwise locations of the added mass influence the fundamental rotating frequencies of the blade to some extent.

Acknowledgments

The work presented in this paper was funded by the European Union Horizon 2020 Program through the project “Shape Adaptive Blades for Rotorcraft Efficiency (SABRE)”, Grant Agreement 723491.

References

1. Maucher, C. K., Grohmann, B. A., and Jäker, P. "Review of adaptive helicopter rotor blade actuation concepts," *Proceedings of the 9th Adaptronic Congress, Göttingen, Germany*, 2005.
2. Friedrich, K. S. "A feasibility study of using smart materials for rotor control," *Smart Materials and Structures* Vol. 5, No. 1, 1996, p. 1.
3. Chopra, I. "Review of State of Art of Smart Structures and Integrated Systems," *AIAA Journal* Vol. 40, No. 11, 2002, pp. 2145-2187.
4. Mistry, M., Gandhi, F., Nagelsmit, M., and Gurdal, Z. "Actuation Requirements of a Warp-Induced Variable Twist Rotor Blade," *Journal of Intelligent Material*

Presented at 44th European Rotorcraft Forum, Delft, The Netherlands, 19-20 September, 2018

Systems and Structures Vol. 22, No. 9, 2011, pp. 919-933.
5. Han, D., Pastrikakis, V., and Barakos, G. N. "Helicopter flight performance improvement by dynamic blade twist," *Aerospace Science and Technology* Vol. 58, 2016, pp. 445-452.
6. Peter, C. C., and Inderjit, C. "Induced strain actuation of composite beams and rotor blades with embedded piezoceramic elements," *Smart Materials and Structures* Vol. 5, No. 1, 1996, p. 35.
7. Chen, P. C., and Chopra, I. "Hover Testing of Smart Rotor with Induced-Strain Actuation of Blade Twist," *AIAA Journal* Vol. 35, No. 1, 1997, pp. 6-16.
8. Chattopadhyay, A., Liu, Q., and Gu, H. "Vibration Reduction in Rotor Blades Using Active Composite Box Beam," *AIAA Journal* Vol. 38, No. 7, 2000, pp. 1125-1131.
9. Carlos, E. S. C., SangJoon, S., and Matthew, L. W. "Dynamic response of active twist rotor blades," *Smart Materials and Structures* Vol. 10, No. 1, 2001, p. 62.
10. Shin, S.-J., and Cesnik, C. "Forward flight response of the active twist rotor for helicopter vibration reduction," *19th AIAA Applied Aerodynamics Conference*. American Institute of Aeronautics and Astronautics, 2001.
11. Dipali, T., and Ranjan, G. "Helicopter vibration reduction in forward flight with induced-shear based piezoceramic actuation," *Smart Materials and Structures* Vol. 13, No. 3, 2004, p. 599.
12. Schultz, M. R. "A Concept for Airfoil-like Active Bistable Twisting Structures," *Journal of Intelligent Material Systems and Structures* Vol. 19, No. 2, 2008, pp. 157-169.
13. Prashant, M. P., and Sung Nam, J. "Active twist control methodology for vibration reduction of a helicopter with dissimilar rotor system," *Smart Materials and Structures* Vol. 18, No. 3, 2009, p. 035013.
14. You, Y. H., Jung, S. N., and Kim, C. J. "Optimal deployment schedule of an active twist rotor for performance enhancement and vibration reduction in high-speed flights," *Chinese Journal of Aeronautics* Vol. 30, No. 4, 2017, pp. 1427-1440.
15. Prahlad, H., and Chopra, I. "Design of a variable twist tilt-rotor blade using shape memory alloy (SMA) actuators," *SPIE's 8th Annual International Symposium on Smart Structures and Materials*. Vol. 4327, SPIE, 2001, p. 14.
16. Bushnell, G. S., Arbogast, D., and Ruggeri, R. "Shape control of a morphing structure (rotor blade) using a shape memory alloy actuator system," *SPIE Smart Structures and Materials + Nondestructive Evaluation and Health Monitoring*. Vol. 6928, SPIE, 2008, p. 11.
17. Ruggeri, R. T., Jacot, A. D., and Clingman, D. J. "Shape memory actuator systems and the use of thermoelectric modules," *SPIE's 9th Annual International Symposium on Smart Structures and Materials*. Vol. 4698, SPIE, 2002, p. 9.
18. Ruggeri, R., Arbogast, D., and Bussom, R. "Wind Tunnel Testing of a Lightweight One-Quarter-Scale Actuator Utilizing Shape Memory Alloy," *49th AIAA/ASME/ASCE/AHS/ASC Structures, Structural Dynamics, and Materials Conference, 16th AIAA/ASME/AHS Adaptive Structures Conference,10th AIAA Non-Deterministic Approaches Conference, 9th AIAA Gossamer Spacecraft Forum, 4th AIAA Multidisciplinary Design Optimization Specialists Conference*. American Institute of Aeronautics and Astronautics, 2008.
19. Clingman, D., and Jacot, D. "Shape Memory Alloy Consortium and demonstration," *41st Structures, Structural Dynamics, and Materials Conference and Exhibit*. American Institute of Aeronautics and Astronautics, 2000.
20. Pagano, A., Ameduri, S., Cokonaj, V., Prachar, A., Zachariadis, Z., and Drikakis, D. "Helicopter blade morphing strategies aimed at mitigating environmental impact," *Jounral of Theoretical and Applied Mechanics* Vol. 49, No. 4, 2011, pp. 1233-1259.
21. Vos, R., Gurdal, Z., and Abdalla, M. "Mechanism for Warp-Controlled Twist of a Morphing Wing," *Journal of Aircraft* Vol. 47, No. 2, 2010, pp. 450-457.
22. Hodges, D. H. "Geometrically Exact, Intrinsic Theory for Dynamics of Curved and Twisted Anisotropic Beams," *AIAA Journal* Vol. 41, No. 6, 2003, pp. 1131-1137.
23. Amoozgar, M. R., and Shahverdi, H. "Analysis of nonlinear fully intrinsic equations of geometrically exact beams using generalized differential quadrature method," *Acta Mechanica* Vol. 227, No. 5, 2016, pp. 1265-1277.

Presented at 44th European Rotorcraft Forum, Delft, The Netherlands, 19-20 September, 2018

24. Amoozgar, M. R., Shahverdi, H., and Nobari, A. S. "Aeroelastic Stability of Hingeless Rotor Blades in Hover Using Fully Intrinsic Equations," *AIAA Journal* Vol. 55, No. 7, 2017, pp. 2450-2460.
25. Sotoudeh, Z., and Hodges, D. H. "Structural Dynamics Analysis of Rotating Blades Using Fully Intrinsic Equations, Part I: Formulation and Verification of Single-Load-Path Configurations," *Journal of the American Helicopter Society* Vol. 58, No. 3, 2013, pp. 1-9.
26. Mardanpour, P., Hodges, D. H., Neuhart, R., and Graybeal, N. "Engine Placement Effect on Nonlinear Trim and Stability of Flying Wing Aircraft," *Journal of Aircraft* Vol. 50, No. 6, 2013, pp. 1716-1725.
27. Yu, W., Hodges, D. H., Volovoi, V., and Cesnik, C. E. S. "On Timoshenko-like modeling of initially curved and twisted composite beams," *International Journal of Solids and Structures* Vol. 39, No. 19, 2002, pp. 5101-5121.
28. Peterson, R. L., Field, M., Johnson, W., and Alto, P. "Aeroelastic loads and stability investigation of a full-scale hingeless rotor," *NASA Technical Memorandum 103867*, 1991.
29. Ong, C. H., and Tsai, S. W. "Design, manufacturing and testing of a bend-twist D-spar," *Stanford University, SAND 99-1324*, 1999.

Presented at 44th European Rotorcraft Forum, Delft, The Netherlands, 19-20 September, 2018